Reprinted from *J. Mol. Biol.* (1975) **98**, 235–242

Beef Liver Catalase Structure: Interpretation of Electron Micrographs

P. N. T. Unwin

J. Mol. Biol. (1975) **98**, 235–242

Beef Liver Catalase Structure: Interpretation of Electron Micrographs

P. N. T. Unwin

Medical Research Council Laboratory of Molecular Biology
Hills Road, Cambridge CB2 2QH, England

(Received 29 April 1975)

It is shown that the catalase platelets frequently examined by electron microscopists have the space group symmetry $P2_12_12_1$ and contain four molecules in the orthorhombic unit cell. The cell dimensions, determined from X-ray diffraction patterns, are: $a = 69$ Å, $b = 173{\cdot}5$ Å, $c = 206$ Å.

Comparison of images of the platelets, prepared in different ways, indicates that the normal negative staining pattern formed by them gives only a very rough, low resolution representation of their native structure.

1. Introduction

Beef liver catalase is a heme-containing enzyme of molecular weight 250,000 (Sumner & Gralen, 1938) made up of four subunits arranged with a point group symmetry of 222 (Kiselev *et al.*, 1968; DeRosier, 1971; Vainshtein, 1973). Conveniently, as far as the electron microscopist is concerned, it can be made to crystallize as platelets which may be several microns across, but only a few hundred angstroms thick. These platelets, negatively stained, have been used extensively for magnification calibration purposes (see, for example, Wrigley, 1968). They have also been the subject of a number of investigations (e.g. Hall, 1950; Valentine, 1964; Labaw, 1967).

There are, however, conflicting ideas about their structure. This is in part brought about, it seems, by over-simplified interpretation of the images formed by the negatively stained specimens. Confusion may also have arisen from the fact that most preparations contain thin crystals of more than one class.

In this paper a solution is given for the molecular packing arrangement of the platelets, based on a comparison of their negatively stained appearance with the negatively stained appearance of single layers of the molecules. Diffraction patterns of the platelets immersed in glucose, where the native configuration of the protein seems to be preserved, and electron micrographs of positively stained specimens support this interpretation. It is also evident from these results that the normal (uranyl) staining procedures affect the catalase molecule in such a way that images of stained specimens can only provide a rough indication of the native structure.

2. Materials and Methods

(a) *Specimen preparation*

The catalase platelets were prepared according to the NaCl dialysis procedure of Sumner & Dounce (1955) from a 2× recrystallized aqueous suspension (Sigma Chemical Co.). Single layer, two-dimensional, sheets were also obtained in this way, by extracting a small portion of the dialysis solution at an early stage of crystal development.

Like most protein crystals, these platelets lose all three-dimensional order when dehydrated directly in the microscope vacuum (e.g. Matricardi *et al.*, 1972). This order can nevertheless be retained, at least to a resolution of 3 to 4 Å, if the water is replaced by glucose or similar less volatile fluid medium (Unwin & Henderson, 1975 and see below). It is also retained (although to a much more limited degree) by conventional staining and embedding methods.

To obtain the "unstained" and the conventional negatively stained preparations, suspensions of the crystals were applied to the microscope grids and washed with a 1% solution of glucose and uranyl acetate, respectively, following the procedure described by Huxley & Zubay, 1960.

Positively stained preparations were made by suspending the crystals in a saturated solution of uranyl acetate in alcohol, after fixation in 1% gluteraldehyde, then replacing the salt solution with a 1% solution of araldite (CY219) in ethyl alcohol before applying the suspension to the grids. Variations of this procedure, using, for example, uranyl acetate in water instead of in alcohol, led to images the optical diffraction patterns of which were the same in character but inferior in resolution.

(b) *X-ray diffraction and electron microscopy*

X-ray diffraction patterns were taken with an Elliott rotating anode tube and point focussing camera (for details, see Henderson, 1975) using CuKα_1 radiation and a specimen-to-film distance of 8 to 10 cm. The focussed spot on the film was $\sim$ 0·05 mm $\times$ 0·15 mm and the exposure time required was 1 to 2 days. For most of the experiments the samples were contained in a wet cell incorporating 2 thin mylar windows. The aqueous medium used was 0·14 M-NaCl. Salt concentrations as high as this were necessary to solubilize the trigonal crystals which otherwise tended to contaminate the patterns.

One of the windows to the wet cell was removed to enable efficient dehydration for the experiments in which glucose was involved.

All electron micrographs and electron diffraction patterns were taken with a Philips EM301 operating at 100 kV. The imaging and electron diffraction of the "unstained" material, where extremely low electron doses are necessary, as well as the image processing methods required for this special case, are described in detail elsewhere (Unwin & Henderson, 1975).

(c) *Processing of data*

The reciprocal spacings of the rings in the X-ray powder patterns were determined by scanning them with an automatic densitometer, circularly averaging over 30° sectors (using a program written by Dr R. A. Crowther) and correcting for the geometry associated with a flat film. The unit cell dimensions were established by searching for the best fit of calculated reciprocal lattice spacings with the reciprocal spacings found for these rings.

"Noise" filtered images of the stained specimens were obtained from electron micrographs by the following steps: (i) selected areas in appropriate micrographs were densitometered, with a step size corresponding to 4 Å, to give 512 $\times$ 512 arrays of optical density readings; (ii) the Fourier transform of each of these arrays was calculated; (iii) the phases and peak amplitudes at the reciprocal lattice points in the transform corresponding to the periodicities in the specimen were collected; (iv) these phases (see also Interpretation section) and amplitudes were recombined by Fourier synthesis giving the final results. Filtering in this way is essentially equivalent to optical filtering using small holes in the mask. The computer programs were developed originally by DeRosier & Klug, 1968 and DeRosier & Moore, 1970, and subsequently modified by Dr L. A. Amos.

Fourier transform data were collected only to a resolution of $\sim$20 Å. At this level of resolution and with the small degrees of defocus applied, it was unnecessary to correct for the effects of non-uniform contrast transfer (see Erickson & Klug, 1971).

The filtered images were assumed to give only qualitative representations of projected densities of the protein and hence were displayed as density plots (Gossling, 1967) rather than in the form of contour maps. For comparison, the more accurate projected structures obtained from the unstained crystals were displayed in the same way and at the same resolution.

Optical diffraction was used in the initial selection of micrographs most suitable for subsequent analysis and for illustrative purposes (Plate III).

3. Results

(a) *X-ray diffraction*

Preliminary X-ray diffraction patterns were taken from crystals which had been oriented, by gentle centrifugation, so that their large flat faces tended to be perpendicular to the X-ray beam. From these "oriented powder patterns" the lattice parameters $a = 69$ Å, $b = 173{\cdot}5$ Å, $\gamma = 90°$ and axial ratio $a/b = 0{\cdot}399 \pm 0{\cdot}002$ were established.

Subsequently, diffraction patterns were taken from randomly oriented crystals (see Plate I). From these, a complete set of indices for all the distinct, low angle rings was found. It required the c-axis to be perpendicular to the a and b axes and that $c = 206$ Å. The crystals are therefore orthorhombic.

Randomly oriented powder patterns were also taken from the catalase crystals under the conditions in which they were to be examined in the electron microscope; that is, immersed in glucose and dehydrated in a vacuum ($\sim 10^{-1}$ torr). These patterns are not as clear as the corresponding aqueous ones, but this is partly due to the stronger diffuse scattering from the glucose (peaking at about 1/5 Å^{-1}) and to the difficulty in creating such high concentrations of crystals in a medium of similar density to the protein.

The two types of powder pattern (compared in Plate I) show good correspondence in the high angle region. The high angle features in X-ray patterns of protein crystals arise mainly from intra-molecular structure and are little affected by the density of the medium in which the protein is immersed. Therefore the good correspondence strongly suggests that the native conformation of the protein is not significantly disturbed by the glucose, at least to the resolution of the X-ray patterns ($\sim$4 Å). In the low angle region (for spatial frequencies of less than, say, 1/12 Å^{-1}) there are marked differences between the two patterns. However, this is only to be expected, since in the low angle region differences between the mean density of the protein and of the surrounding medium become important (see e.g. Bragg & Perutz, 1952). The density of non-crystalline glucose ($\sim 1{\cdot}4$ g/cm^3) is very close to that of protein ($\sim 1{\cdot}3$ g/cm^3) so that the low angle reflections tend to be weaker, on the whole, in the glucose pattern than they are in the aqueous pattern.

Because of the exact correspondence between the two patterns at high angles, the same unit cell dimensions and axial ratios must apply for the glucose case as for the aqueous case. Indeed, no significant change in these parameters could be detected by measurement of electron diffraction patterns from catalase in glucose (see below).

(b) *Electron microscopy*

The results below concern the projection of the molecules onto the plane in which the a and b axes lie.

(i) *Unstained crystals*

Images of these do not display periodicities apparent to the eye because of the inherently low contrast and the statistical noise associated with the low electron dose at which they need to be taken. Therefore, rather than the micrograph, a (low angle) electron diffraction pattern is illustrated (Plate III(a)). It has *mm* symmetry and alternate reflections along the two axial directions are systematically absent to high resolutions (see Plate I, Unwin & Henderson, 1975), indicating the presence

of two mutually orthogonal 2-fold screw axes. The crystals therefore have the orthorhombic space group $P2_12_12_1$ or $P2_12_12$.

A low resolution projection calculated from electron diffraction intensities as in Plate III(a), using phases computed from the images (Unwin & Henderson, 1975), is shown in Plate IV(a). Its plane group symmetry is *pgg*. The convention for all such displays is that regions of more weakly scattering matter appear darker.

The (dark) more weakly scattering regions in this projection are interpreted to be the regions consisting mainly of protein. This is because at low resolution the contrast arises mainly from the difference between the mean density of the protein and that of the surrounding medium, and the mean density of the protein is lower than that of the glucose.

The appearance of this projection (or equivalently, of the electron diffraction pattern) is extremely sensitive to electron dose. It has been studied in detail by carrying out Fourier syntheses using the dose-affected electron diffraction intensities (Unwin, unpublished results) and the centrosymmetric phases for the undamaged structure. It changes very rapidly over the dose range 0 to 1 electron/Å^2 but then stabilizes, presumably because of radiation-induced cross-linking reactions, forming the pattern shown in Plate IV(b).

(ii) *Negatively stained crystals*

An image and optical diffraction pattern of a negatively stained crystal are shown in Plates II(a) and III(b). These images, and indeed all those from stained specimens, are considerably less sensitive to electron dose effects than are those of the unstained specimens; the irradiation causes only a gradual weakening of the (originally much poorer) electron diffraction pattern and does not produce very marked changes in the relative intensities of reflections of similar resolution.

To calculate the filtered image corresponding to Plate II(a), the phase origin in its Fourier transform was refined to minimise the discrepancy between the observed phases and the nearest real values which would apply for true *pgg* symmetry. This gave a root-mean-square error for individual measurements of phase of 25°. The filtered image (Plate IV(c)) was then computed by setting all the phases to their nearest real values. The weak "forbidden" (1,0) reflection evident in Plate III(b) was not included in the computations.

(iii) *Positively stained crystals*

These look remarkably different to their negatively stained counterparts, although (as the optical diffraction pattern, Plate III(c), shows) the same lattice dimensions apply to either case. A typical micrograph is shown in Plate II(b) and the corresponding filtered image, computed in the same way as for the negatively stained crystal, is shown in Plate IV(d).

(iv) *Two-dimensional arrays*

An image and optical diffraction pattern of a negatively stained two-dimensional array of catalase molecules—from which it is likely that these three-dimensional crystals are built up—are shown in Plates II(c) and III(d). The borders of the array in Plate II(c) appear to be distorted, and in many images of such arrays these distortions appeared to continue even into the central regions. Since the a/b axial ratio in the optical diffraction pattern of this array is 0·402, corresponding closely to the

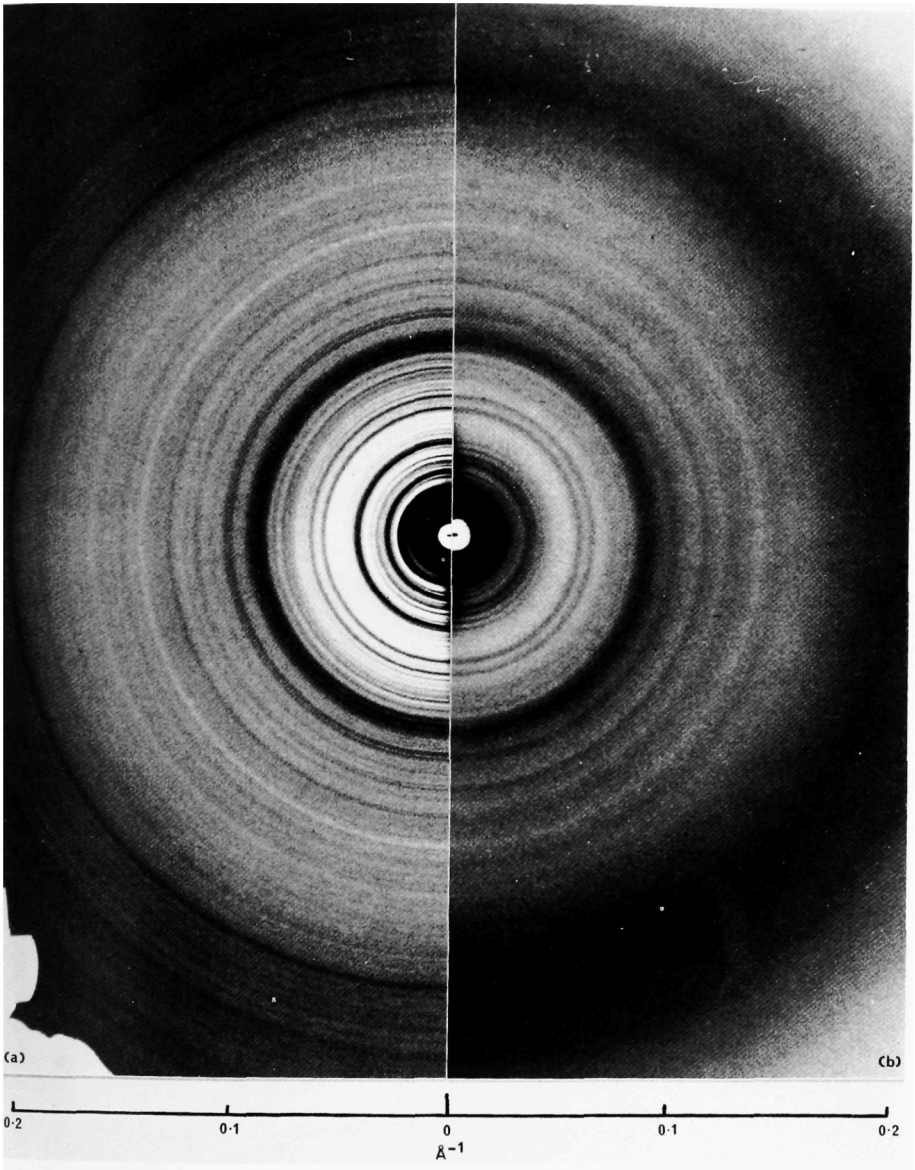

PLATE I. X-ray powder patterns from catalase platelets (a) in 0·8% NaCl and (b) in dehydrated glucose. The band of strong diffuse scattering in (b) is due to the glucose; the high angle powder rings can be seen to match up closely in their positions and intensities, indicating that the protein conformation is not significantly disturbed when the aqueous solution is replaced by glucose.

[*facing p. 238*

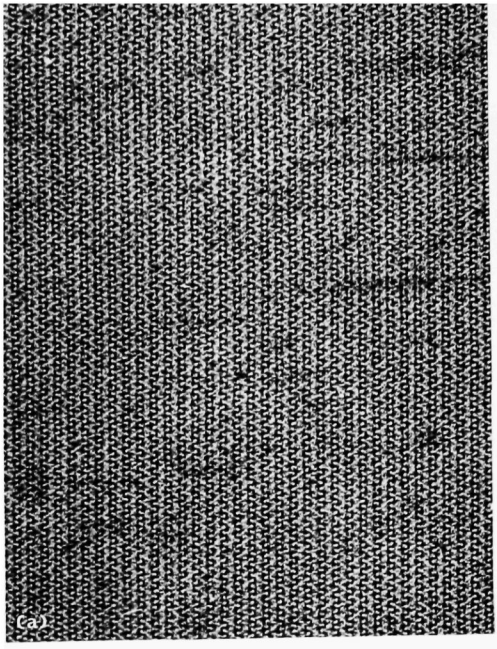

Platelet, negatively stained

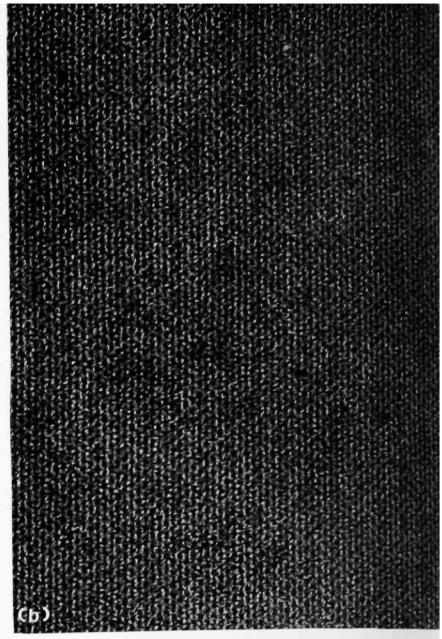

Platelet, positively stained

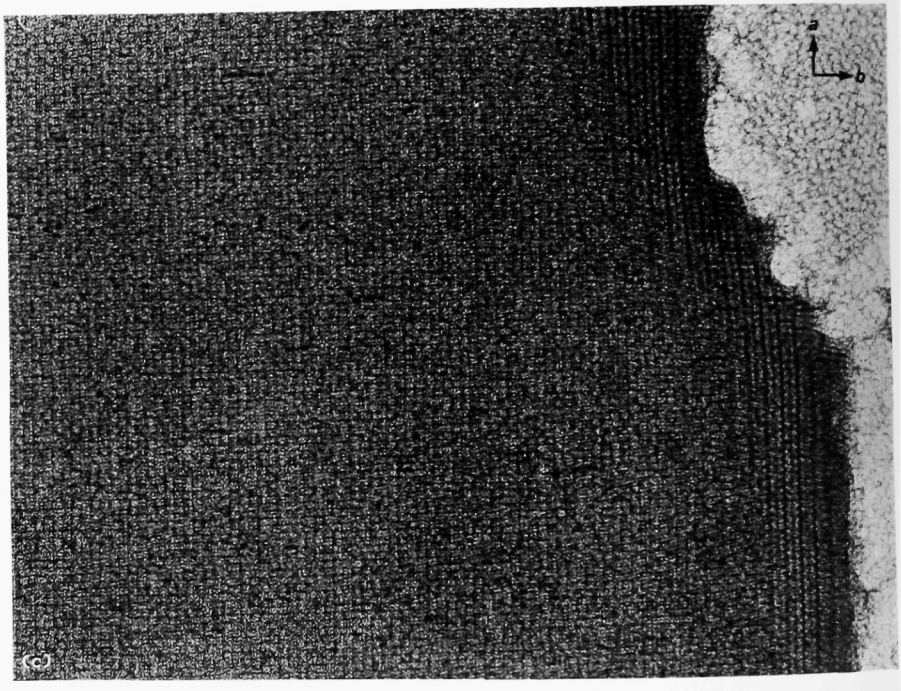

Single layer, negatively stained

PLATE II. Electron micrographs of (a) a negatively stained platelet; (b) a positively stained platelet and (c) a negatively stained single layer of catalase molecules. Two facts argue against the possibility that regions having the appearance of (c) are actually platelets comprised of several layers, only part of which is strongly stained. One is that regions having this appearance can only be obtained after interrupting the dialysis at a very early stage. The other is that the boundaries between these regions and regions of randomly oriented molecules are often indistinct. The stain used was uranyl acetate. Focussing was carried out on regions adjacent to the specimens so that minimal electron doses were used in recording the micrographs. Magnifications: (a), (b) 235,000 × ; (c) 305,000 × .

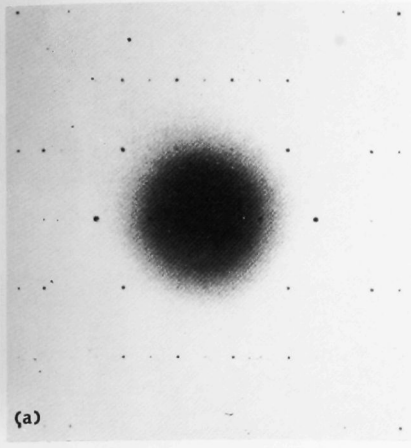

Platelet, unstained

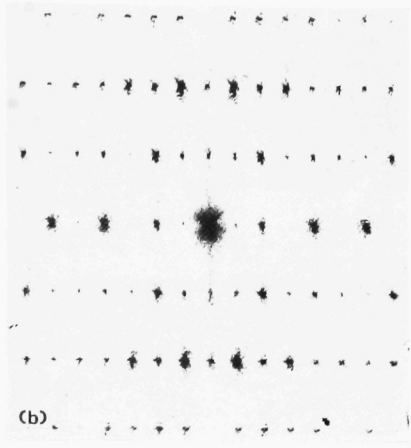

Platelet, negatively stained

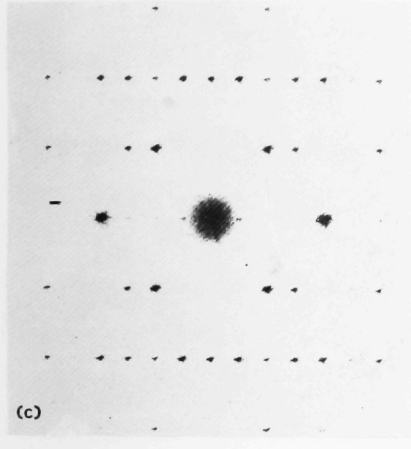

Platelet, positively stained

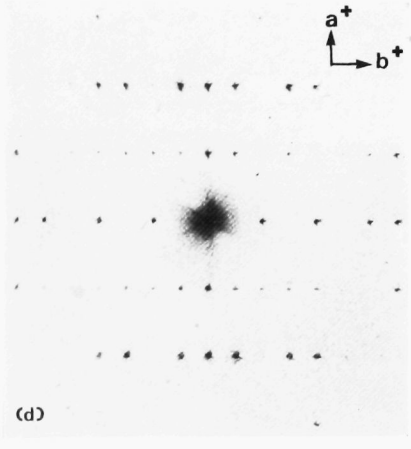

Single layer, negatively stained

PLATE III. (a) Electron diffraction pattern from unstained catalase, preserved in glucose and recorded with a low electron dose ($<0{\cdot}1$ electrons/Å^2). (b), (c) and (d) optical diffraction patterns from the micrographs in Plate II(a), (b) and (c) respectively. Scale: 1 cm = 1/70 Å^{-1}.

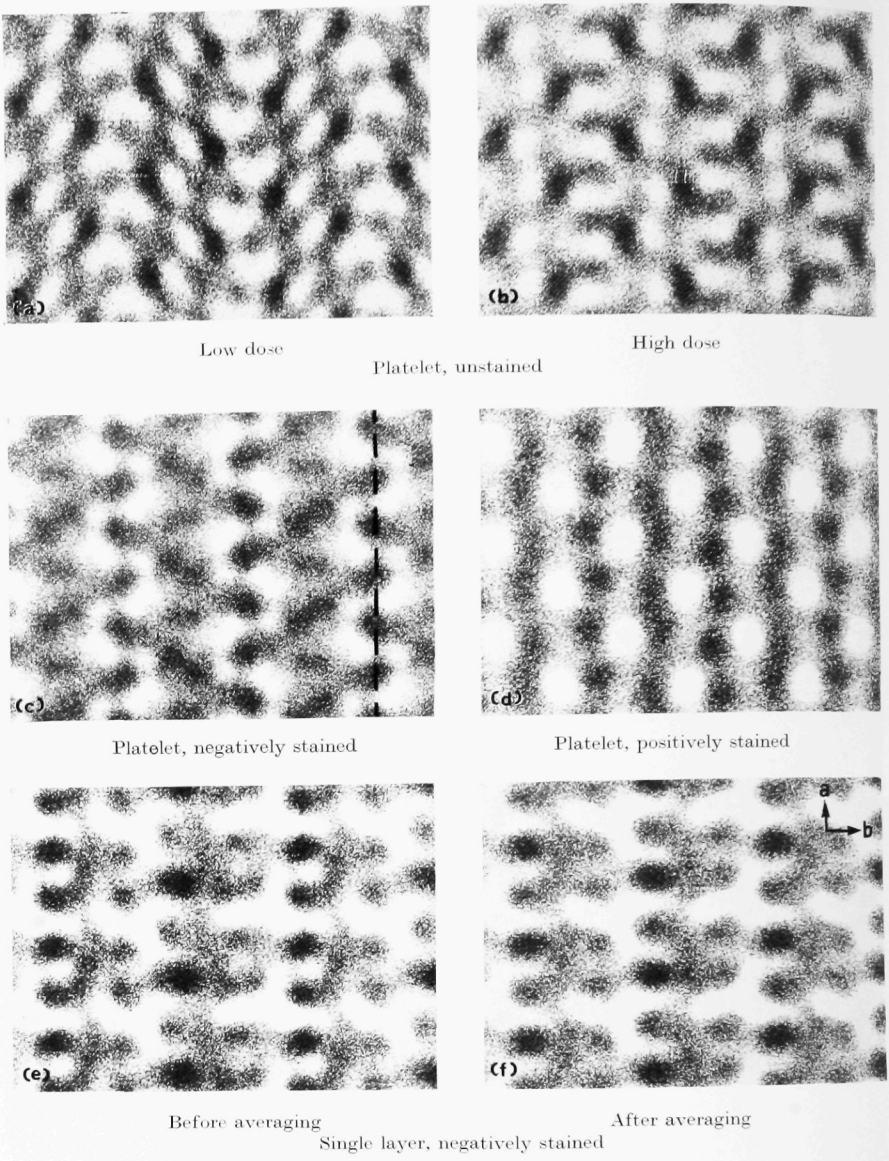

Low dose — High dose

Platelet, unstained

Platelet, negatively stained — Platelet, positively stained

Before averaging — After averaging

Single layer, negatively stained

PLATE IV. 20 Å resolution density displays computed from electron micrographs (or, (a) and (b), combined micrograph–electron diffraction data).

(a) The projected structure of unstained catalase at an electron dose level ($\sim 0{\cdot}1$ electron/Å^2) insufficient to damage the protein significantly; (b) the projected structure after it has been "stabilized" by radiation damage (dose ~ 7 electron/Å^2); (c) and (d) filtered images of the negatively stained and positively stained platelets, respectively; (e) and (f) filtered images of the single layer before (e) and after (f) averaging on the assumption that there is a *b* glide plane present. The broken lines in (e) and in Plate VI are in equivalent positions (see text).

The darker regions represent higher concentrations of more weakly scattering matter. In (a) and (b) this is the protein; in (c), (e) and (f) this is the protein that is not positively stained; and in (d) this is any region where little or no positive stain is present.

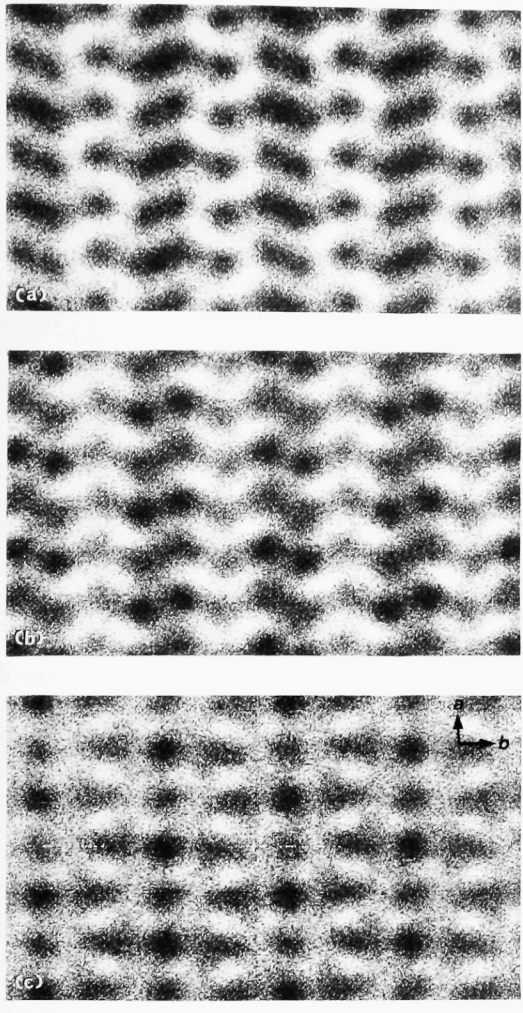

PLATE V. Superposition "images" formed by packing the negatively stained single layers of molecules so that the lattice formed by every odd layer is rotated 180° and shifted half the axial spacing in the a direction with respect to that of every even layer. The relative displacement along the b direction is varied.

(a) Shows optimum correlation with the filtered image of the negatively stained crystal (correlation coefficient = 0·57). It corresponds to the situation where the centres of the molecules in the odd layers are in the body-centred positions of the lattice formed by the centres of the molecules in the even layers (see Plate VI). (b) and (c) are formed by relative displacement of the two layers by +15 Å and −15 Å from their positions in (a) (correlation coefficient = 0·33 in each case).

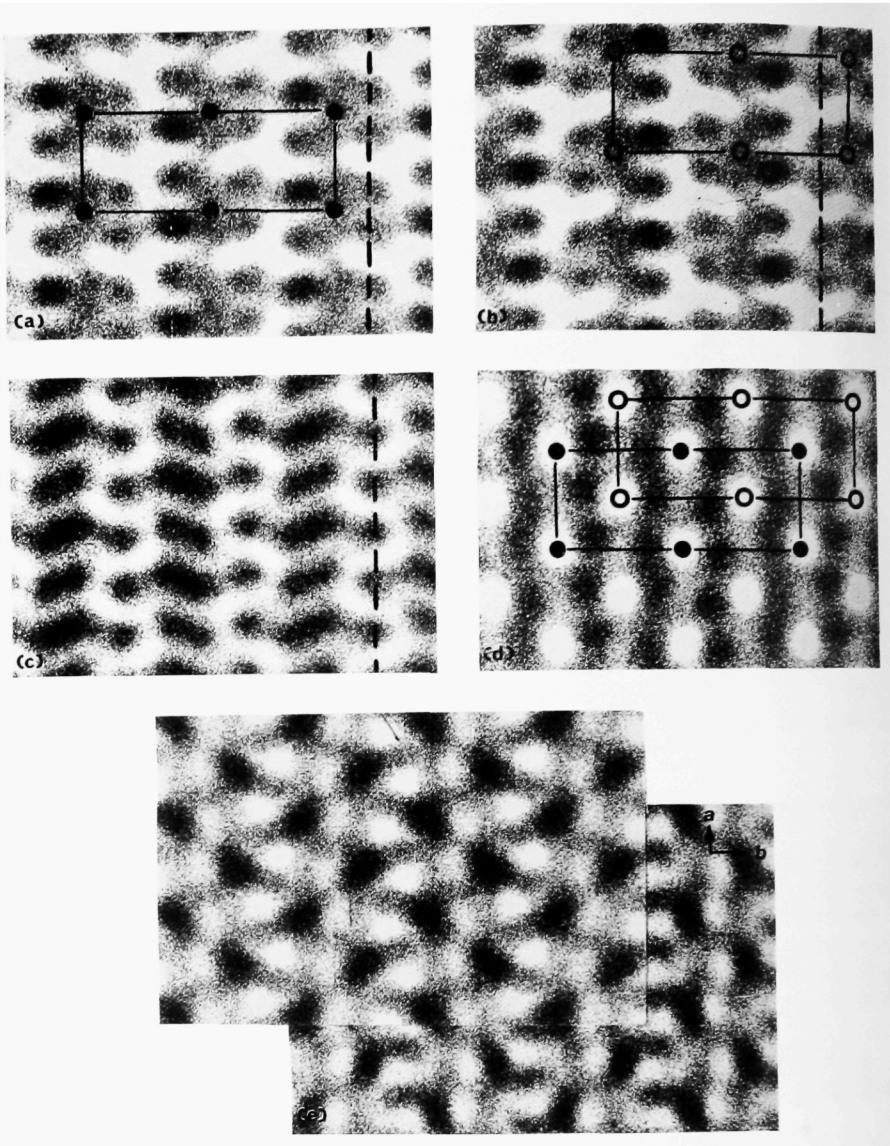

PLATE VI. Interpretation of the patterns in Plate IV. (a) and (b) are the single layers in relative orientations such that when superposed they form a pattern, (c), correlating closely (see Plate V) with that formed by the negatively stained three-dimensional crystal (Plate IV(c)). Thus the density distribution along the broken line either in (c) or in Plate IV(c) arises from superposition of the extremities of the molecules, and so on. (d) Is the filtered image of the positively stained crystal: the (white) regions of high concentration of positive stain form the same projected lattice as that formed by the centres of the molecules when superposed as in (c). (e) (upper part) is an "image" formed by subtracting out the positively stained regions, indicated by (d), from the negative stain pattern (Plate IV(c)). This involved subtraction of one Fourier transform from the other, having the ratio of the sums of the structure factor amplitudes, $\sum|F|_{\text{negative stain}}/\sum|F|_{\text{positive stain}}$, equal to 3. The "image" is very similar to the projection of the radiation damaged, unstained crystal (lower part). This correspondence does not depend critically on the relative weights applied to the Fourier transforms.

X-ray figure of 0·399 for the three-dimensional crystals (the axial ratios in cases (ii) and (iii) are also within 3% of this figure), it is reasonable to assume that there is a minimum degree of distortion present in this particular example.

The filtered image computed directly from the micrograph in Plate II(c), Plate IV(e), has a peculiar appearance, probably brought about by residual distortions and by uneven staining of the top and bottom parts of the molecules. It does however have an approximate *b* glide line of symmetry, and assuming that an undistorted and uniformly stained single layer has strict glide symmetry in projection, the best estimate of the projected views of the molecule is obtained by averaging using this symmetry constraint. The result is shown in Plate IV(f). Its plane group symmetry (*pg*) suggests that the 2-fold screw axes of the three-dimensional crystal, which give rise to its projected *pgg* symmetry, are non-intersecting and hence that the space group of the crystal is $P2_12_12_1$.

4. Interpretation

It is easy to construct a model comprised of four elongated subunits arranged with 222 symmetry which, in projection, would resemble each patch of density in Plate IV(f). In these quaternary features, and scaled to the observed projected area of 90×70 Å^2, such a model aptly fits recent descriptions of the catalase molecule (Kiselev *et al.*, 1968; Barynin & Vainshtein, 1972). Each patch of density in Plate IV(f) is therefore interpreted to be a single molecule (there being two such molecules in the unit cell).

Unfortunately, this representation of the molecule is not likely to be an accurate one. An important reason for this, made evident by Plate IV(e) in particular, is that the preparation procedure introduces distortions which can only partially be eliminated by applying symmetry constraints. The same problem arises, of course, with the other filtered images and is compounded in the case of the thicker negatively stained crystals by the fairly important effects of multiple electron scattering (Voter & Erickson, 1974).

Despite these difficulties, one might hope to derive a superposition pattern from the single layer of molecules which would bear a close enough resemblance to the pattern formed by the negatively stained crystal to establish their three-dimensional packing arrangement.

The most likely type of arrangement which satisfies the *pgg* symmetry requirement of the three-dimensional crystal in projection is that derived by alternating the packing of the single layer so that the lattice formed by every odd layer is rotated by 180° about the *c*-axis and shifted half the axial spacing in the *a* direction with respect to that of every even layer. The odd layers (and the even layers) should also superpose directly when projected down the orthogonal *c*-axis. The symmetry is maintained, however, independently of the relative displacement between the odd and the even layers in the *b* direction. This relative displacement has to be worked out.

Trial superposition "images" were therefore generated for various displacements between odd and even layers in the *b* direction, and correlated numerically with the filtered image of the three-dimensional negatively stained crystal (see Plate V). The procedure involved addition of the single layer Fourier transforms (taking account of the orientation differences) and Fourier synthesis of the resultant transforms. This approach is only an approximate one, since the Fourier transform of an image of a

specimen several layers thick is not exactly equal to the sum of the Fourier transforms of the individual layers (Cowley & Moodie, 1957). However, the approximation does apply reasonably well to negatively stained specimens at low resolutions (e.g. DeRosier & Klug, 1972) and should be adequate for the present purpose.

A unique superposition "image" having the character of the filtered image of the three-dimensional negatively stained crystal was found when the relative displacement was such that the centres of the molecules in the odd layers were in the body-centred positions of the lattice formed by the centres of the molecules in the even layers (see Plate VI). There are inevitable differences of detail between the two (compare Plate IV(c) and Plate V(a) or VI(c)), but the similarity of the low resolution features is quite striking. Thus the same "staircase" pattern can be identified in either case; along common lines, e.g. the one indicated in Plate VI (which is due to the superposition of the extremities of the molecules), similar superposition effects are observed, and so on.

The three-dimensional packing arrangement now arrived at is consistent with the space group $P2_12_12_1$, with four molecules per unit cell. The glide line present in the projection of a single layer is equivalent to the 2-fold screw axis parallel to b, and the alternate layers are packed so as to be related by 2-fold screw axes parallel to a and c.

This solution of the packing arrangement leads to a very simple explanation for the positive staining pattern, since the lattice generated in projection by the centres of the superposed molecules is the same as that generated by the high concentrations of positive stain (see Plate VI(d)). This means that either the central regions of the molecules or the regions midway between the molecules in the a direction are preferentially positively stained. The former alternative is, of course, the most likely in practice.

Given that the positive stain does concentrate at the centres of the molecules, there are two possibilities for the relative positioning of the positive and negative stain patterns in Plate IV(c) and (d): as shown (relative, say, to a common corner in each display) or with one pattern shifted half a unit cell spacing with respect to the other along the b direction. It is not possible to distinguish between these alternatives. An interesting pattern is obtained, however, by subtraction of the Fourier transform for the positive stain pattern from that for the negative stain pattern in the relative orientations shown. It bears a striking likeness to the pattern formed by the radiation damaged unstained crystal (see Plate VI(e)).

Subtraction of the two Fourier transforms in the above way should be equivalent to replacement of the positively stained regions in the negatively stained crystal by "protein". The manipulations involve weighting factors which, although realistic (see the legend to Plate VI(e)), are somewhat arbitrary and may therefore exaggerate the likeness which would be achieved if the true weighting factors were known. Nevertheless, the fact that a close correspondence with the unstained crystal pattern *can* be obtained by such a subtraction procedure strongly suggests that the negative stain does positively stain the molecules as well, and that this effect needs to be corrected for to obtain a more realistic projected structure. That negative staining can contribute both a "negative" and a "positive" component has been found in studies of other materials, e.g. nucleoproteins (see Valentine, 1961).

In summary, there is a qualitative relation between the images of the positively and negatively stained crystals, the images of the negatively stained single layer of

molecules and the image formed by the radiation damaged unstained crystals. The undamaged unstained structure apparently does not correlate directly with any combination of these.

5. Discussion

The qualitative relation found between the conventionally prepared crystals and the radiation-affected unstained crystals (Plate VI) should be considered in the light of their differences in behaviour under irradiation (see Results). The electron diffraction patterns of the stained crystals, in contrast to those of the unstained crystals, do not extend initially to high resolution and change relatively slowly with electron dose. At 20 Å resolution they are virtually the same at any dose up to that used in recording the micrograph. This suggests that at doses where the protein is not significantly damaged by irradiation, the stained specimens are already altered as if they had been irradiated. In other words, it seems that the gross changes in protein structure brought about by the conventional preparation procedures, or by the subsequent dehydration, are of the same nature as those produced by initial irradiation of the "native" protein. This is a reasonable result, since the denaturing conditions set up in either case, although of entirely different character, might well preferentially affect the same sensitive parts of the molecule.

Alterations of the catalase molecule due to the preparation method may be closely connected with the observed strong positive staining effect. But this is difficult to prove.

In any event, either effect would clearly lead to inaccuracies of sufficient magnitude to produce significant differences between the low angle X-ray and electron microscopic data. In the case of the trigonal crystals, where direct comparison is available, significant low resolution differences are indeed present (see e.g. Longley, 1967, Plates II and III; Gurskaya *et al.*, 1972, Fig. 1). It is also notable that the model of the catalase molecule constructed by Vainshtein and his colleagues, using X-ray diffraction intensities, has a "more compact" structure than the model constructed from images of the negatively stained crystals (Gurskaya *et al.*, 1972). Since the positive staining reaction appears to affect preferentially the central region of the molecules, that is a result this investigation predicts.

6. Conclusion

The beef liver catalase platelets commonly studied by electron microscopists have a space group symmetry $P2_12_12_1$ and contain four molecules in the orthorhombic unit cell.

Negative staining of these platelets (with uranyl salts) leads only to a rough low resolution picture of the projected structure, because of simultaneous positive staining effects and because the native configuration of the molecules is altered slightly as a result of the preparation method, before they are observed.

I thank Drs J. T. Finch, R. A. Crowther and R. Henderson for help.

REFERENCES

Barynin, V. V. & Vainshtein, B. K. (1972). *Sov. Phys. Crystallogr.* **16**, 653–661.
Bragg, W. L. & Perutz, M. F. (1952). *Acta Crystallogr.* **5**, 277–283.
Cowley, J. M. & Moodie, A. F. (1957). *Acta Crystallogr.* **10**, 609–619.

DeRosier, D. J. (1971). *Phil. Trans. Roy. Soc. ser. B*, **261**, 209–210.
DeRosier, D. J. & Klug, A. (1968). *Nature (London)*, **217**, 130–134.
DeRosier, D. J. & Klug, A. (1972). *J. Mol. Biol.* **65**, 469–488.
DeRosier, D. J. & Moore, P. B. (1970). *J. Mol. Biol.* **52**, 355–369.
Erickson, H. P. & Klug, A. (1971). *Phil. Trans. Roy. Soc. ser. B*, **261**, 105–118.
Gossling, T. H. (1967). *Acta Crystallogr.* **22**, 465–468.
Gurskaya, G. V., Lobanova, G. M. & Vainshtein, B. K. (1972). *Sov. Phys. Crystallogr.* **16**, 662–669.
Hall, C. E. (1950). *J. Biol. Chem.* **185**, 749–754.
Henderson, R. (1975). *J. Mol. Biol.* **93**, 123–138.
Huxley, A. & Zubay, G. (1960). *J. Mol. Biol.* **2**, 10–18.
Kiselev, N. A., DeRosier, D. J. & Klug, A. (1968). *J. Mol. Biol.* **35**, 561–566.
Labaw, L. W. (1967). *J. Ultrastruct. Res.* **17**, 327–341.
Longley, W. (1967). *J. Mol. Biol.* **30**, 323–327.
Matricardi, V. R., Moretz, R. C. & Parsons, D. F. (1972). *Science*, **177**, 268–269.
Sumner, J. B. & Dounce, A. L. (1955). *Meth. Enyzmol.* **II**, 775–781.
Sumner, J. B. & Gralen, N. (1938). *J. Biol. Chem.* **125**, 33–36.
Unwin, P. N. T. & Henderson, R. (1975). *J. Mol. Biol.* **94**, 425–440.
Vainshtein, B. K. (1973). *Usp. Fiz. Nauk.* **109**, 455–549.
Valentine, R. C. (1961). *Advan. Virus Res.* **8**, 287–318.
Valentine, R. C. (1964). *Nature (London)*, **204**, 1262–1264.
Voter, W. A. & Erickson, H. P. (1974). In *Proc. 32nd Annual Meeting EMSA* (Arceneaux, C. J., ed.), pp. 400–401, Claitor's Publishing Division, Baton Rouge, U.S.A.
Wrigley, N. G. (1968). *J. Ultrastruct. Res.* **24**, 454–464.